



# Simulating energy consumption based on material addition rates for material extrusion of CFR-PEEK: a trade-off between energy costs and cycle time

Mohammad Rashidul Hassan<sup>1</sup> · Heena Noh<sup>2</sup> · Kijung Park<sup>2</sup> · Hyun Woo Jeon<sup>3</sup>

Received: 21 November 2021 / Accepted: 21 February 2022 / Published online: 18 March 2022  
© The Author(s), under exclusive licence to Springer-Verlag London Ltd., part of Springer Nature 2022

## Abstract

While many studies for material extrusion-based additive manufacturing (AM) of polymers focus on experimental approaches to evaluate relevant performance measures from process parameters, there is a lack of discussion to connect experimental results with useful applications. Also, one of the major deficiencies in the application literature is a trade-off analysis between energy costs and cycle time (time to produce an item from the beginning to the end) since improving these two measures simultaneously is challenging. Thus, this paper proposes an energy simulation method for performing a trade-off analysis between energy costs and cycle time using combinations of major AM process parameters for material extrusion. We conduct experiments using carbon fiber-reinforced poly-ether-ether-ketone (CFR-PEEK), which is increasingly used in material extrusion. From experimental results, we build a power model in which power (kW) is derived as a linear function of material addition rates (MAR). This MAR regression model is then used in a proposed simulation model that integrates discrete event simulation and numerical simulation. In our simulation case study of 50 machines and 40 scenarios, we investigate trade-offs between energy costs and cycle time with three control policies ( $P_1$ ,  $P_{25}$ , and  $P_{50}$ ) that allow 1, 25, or 50 machines to start heating, respectively. The trade-off analysis results show that  $P_{25}$  can be preferred when a balance between cycle time and energy costs is pursued, while  $P_1$  or  $P_{50}$  can be chosen if either energy cost (with  $P_1$ ) or cycle time (with  $P_{50}$ ) is more important than the other measure. Moreover, we find that the machine utilization, variability, and product volume have significant effects on energy costs and cycle time.

**Keywords** Material addition rate · Energy simulation · Energy cost · Cycle time · Trade-off

## 1 Introduction

Additive manufacturing (AM) is a manufacturing technology increasingly used for various applications. In AM, a computer-aided design (CAD) model is created first and then manufactured by depositing a material layer by layer [1]. One major benefit of the AM process is that the manufacture of a three-dimensional (3D) object is relatively quick compared to that in the traditional manufacturing process [2]. AM methods that are broadly used include laser powder bed fusion (LPBF), vat photo-polymerization (VPP), material jetting, and material extrusion [3]. Of these methods, material extrusion is growing in popularity. Industrial sectors such as the automotive, aerospace, and biomedical equipment industries have heavily invested in adopting material extrusion due to its numerous advantages [4].

In studies of AM, sustainable AM is one of the most active research topics. Despite the ongoing global COVID-19

✉ Hyun Woo Jeon  
hwjeon@khu.ac.kr

Mohammad Rashidul Hassan  
mhassa5@lsu.edu

Heena Noh  
nhn@inu.ac.kr

Kijung Park  
kjpark@inu.ac.kr

<sup>1</sup> Department of Mechanical and Industrial Engineering, Louisiana State University, 3261 Patrick F. Taylor Hall, Baton Rouge LA 70803, USA

<sup>2</sup> Department of Industrial and Management Engineering, Incheon National University, 119 Academy-ro, Yeonsu-gu, Incheon 22012, Republic of Korea

<sup>3</sup> Department of Industrial and Management Systems Engineering, Kyung Hee University, 1732 Deogyong-daero, Yongin-si 17104, Republic of Korea

pandemic, the additive manufacturing industry expanded by 7.5% to roughly \$12.8 billion in 2020 [5]. The use of 3D printers increased by 48% in 2020 compared to 2018, with sales of about 2.1 million 3D printers worldwide [6]. Also, 15.3 million units of 3D printers are predicted to be sold by 2028. Correspondingly, a significant rise in the energy consumption (EC) and related electricity costs of AM facilities is likely to occur in upcoming years.

Electricity costs in manufacturing mainly consist of an energy charge and a demand charge for each billing period [7]. An energy charge is calculated using total EC in kilowatt hours (*kWh*), while a demand charge is calculated using the peak power demand in kilowatts (*kW*) [8]. Thus, it is important to clearly understand the dynamics of the total kWh and peak kW during printing in order to keep energy costs lowered in an AM system.

Existing studies of material extrusion largely focused on process parameter optimization [9, 10]. Also, a considerable number of studies have conducted experiments to observe the effect of important AM process parameters on energy performances. For example, the effects of build orientations [11–13], part geometry [11], layer thickness [12–17], printing speed [14, 17], and infill percentages [18, 19] on EC have been well investigated. The majority of those studies, however, only perform experiments [11–17] that show the relationship between process parameters and performance measures in a summarized model without suggesting specific applications. For example, various regression [16], statistical [17], and mathematical [13, 20] studies have suggested equivalent specific energy consumption (SEC) models or material addition rate (MAR) models based on AM parameters. These studies, however, do not consider useful applications that can be made based on their experiments. An energy simulation method can estimate peak kW and total kWh from AM parameters that are not readily available in analytical studies [21]. Relevant studies demonstrate that EC drops, and average cycle time (time to complete processing a part from the start to the end of the process) rises at lower machine utilization [22]. Thus, applications of AM energy models, such as those that consider the various trade-offs between average cycle time and EC, would be beneficial to both industrial practitioners and academic scholars.

Performance measures of material extrusion are largely impacted by the selection of feedstock [23]. Frequently used feedstocks such as acrylonitrile–butadiene–styrene (ABS) and polylactide (PLA) have been extensively studied. In recent years, carbon fiber–reinforced poly-ether-ether-ketone (CFR-PEEK) has emerged as another option, as parts printed using CFR-PEEK exhibit superior mechanical properties when compared to ABS and PLA [24, 25]. Despite the advantages of CFR-PEEK, parts printed using it require additional time to finish printing [26] and thereby increase EC. A few studies investigate the relationship among AM process parameters,

the manufacturing performance [26, 27], and the optimal mechanical properties [28, 29] of CFR-PEEK parts. However, studies that examine the effects of process parameters on energy performances and the productivity of material extrusion using CFR-PEEK are limited.

Various studies suggest that power demand during material removal processes such as milling, turning, and drilling processes can be estimated from material removal rates (MRR). The power demand of a machine consists of the minimum fixed power required to run the machine and the variable cutting power necessary for material removal [30, 31]. Hence, average power (*W*) can be written as  $W = b_0 + b_1 \times MRR$ , where  $b_0$  and  $b_1$  are constants. SEC of a machine tool can also be characterized using MRR [31]. Thus, MRR is applied as an important parameter during the energy study of material removal processes. Similarly, MAR can be considered for AM processes to calculate the power demand of machines.

An energy model using MAR can be integrated with a simulation model to calculate performance measures of material extrusion. MAR can be calculated from build time, as MAR is inversely related to build time. Zhu et al. [32] proposed build time models based on both the parametric and experimental methods by considering volume, height, and density as printing parameters of material extrusion. Komineas et al. [33] demonstrated a model to estimate build time by applying a trapezoidal velocity profile, taking into account the effects of acceleration and deceleration during the extruding nozzle movement as well.

Trade-off analyses between AM performance measures can be crucial to manufacturers with regard to operational perspectives. Park et al. [26] showed that the printing time was lowest for a 0.3-mm layer thickness, while dimensional accuracy and material costs were relatively higher. Kose et al. [34] studied the trade-off between productivity and part quality to optimize various process parameters in a powder bed–based AM process. Previous studies in subtractive manufacturing widely discussed the key trade-offs among average cycle time, EC, and energy costs [35, 36]. However, the trade-off between energy performances and average production cycle time has received less attention in the prevalent AM research.

To address and bridge the aforementioned research gaps, we propose an energy simulation approach to analyze trade-offs between average cycle time and energy costs based on experimental results. More specifically, we conducted a set of experiments in which a specimen was printed to estimate power as a function of material extrusion process parameters. To build a material extrusion power model, we used MAR as a process parameter instead of individual material extrusion process parameters because MAR can represent multiple material extrusion process parameters as a single compound variable. For feedstock, we used CFR-PEEK,

which is increasingly used in various disciplines. Based on the experimental results, material extrusion power was then modeled as a regression equation in which power was written as a function of MAR. To provide an application of MAR regression models, a hypothetical AM facility with 50 parallel material extrusion machines was simulated. In this simulation, discrete event simulation (DES) and numerical simulation methods were combined so that time series power profiles could be generated at the equipment and facility levels for all simulated scenarios. Simio [37] was used to perform DES, and MATLAB [38] was used to conduct a numerical simulation in this study. Then, average cycle time and relevant energy performance measures such as peak kW, total kWh, and associated energy costs were calculated for each scenario. For the simulation, we also proposed a new control policy for material extrusion to reduce the peak kW during heating by limiting the number of machines in that state. Finally, we analyzed an important trade-off between average cycle time and energy costs from experimental and simulation results. Our work can contribute to industrial as well as academic communities by providing a simulation tool that can help manufacturers and researchers find a balance between the average cycle time and energy costs to reduce the overall production costs of AM facilities.

## 2 Material and methods

### 2.1 AM power

A sample energy profile of material extrusion during the three states of heating, building, and cooling is presented in Fig. 1. This energy profile was obtained using the Apium P220 [39] as a material extrusion machine for fabricating CFR-PEEK products ( $2 \times 1 \times 1 \text{ cm}^3$ ) with a layer thickness of 0.1 mm and print speed of 1,000 mm/min. The feedstock employed in our experiment was TECAPEEK CF30 [40, 41], an industrial-grade CFR-PEEK filament compatible

with the Apium P220 printer. The figure shows an example of power measured by Wattman HPM-100A power meter logger [42] for each time point in the time horizon and demonstrates the average power of the material extrusion machine in each of the three states. In heating, the first state, the machine increases the temperature to a certain level on the build platform and extruding nozzle and then maintains it. In building, the second state of material extrusion, the extruded materials are deposited in layers by the extruding nozzle. Finally, in cooling, the third state, the printed product is cooled down and further processed into a finished product.  $W_h$ ,  $W_b$ , and  $W_c$  represent the average power in the heating, building, and cooling states, respectively. Note that power demands during the heating and cooling states barely change over time. Therefore, we assumed that the power demands during those two states were constant in this study.

### 2.2 AM power models with MAR

#### 2.2.1 Process parameters

In this study, we analyzed the average power of material extrusion machines by considering two process parameters: layer thickness and printing speed. We focused on these two process parameters because we believed that they would considerably influence the performance measures of material extrusion machines [18]. Five different layer thicknesses (0.1, 0.15, 0.2, 0.25, and 0.3 mm) and six different printing speeds (1000, 1100, 1200, 1300, 1400, and 1500 mm/min) were considered in our experiments. Table 1 shows the different levels of layer thickness and printing speed, as well as other fixed process parameters, used in our experiments.

#### 2.2.2 Specimen modeling and fabrication

The single test specimen used in our experiments has dimensions of 2-cm length (A), 1-cm width (B), and 1-cm height (C). To compare the energy performance of material

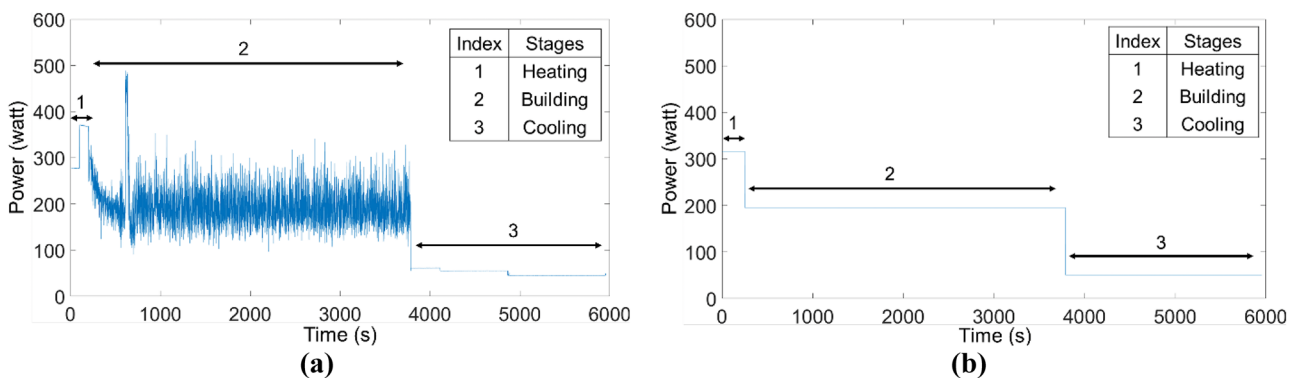


Fig. 1 States of a material extrusion machine with (a) instantaneous and (b) average power for one printing cycle

**Table 1** Process parameters in the experiments

	Level 1	Level 2	Level 3	Level 4	Level 5	Level 6
Variable process parameters						
Layer thickness	0.1	0.15	0.2	0.25	0.3	-
Printing speed	1,000	1,100	1,200	1,300	1,400	1,500
Fixed process parameters						
Build platform temperature	120 °C					
Nozzle temperature	510 °C					
Nozzle diameter	0.4 mm					
Perimeter shells	3					
Number of top layers	0					
Number of bottom layers	0					
Infill pattern	Rectilinear					
Infill percentage	100%					
Infill angle	+45° – 45°					
Extrusion multiplier	96%					
First layer height	90%					
First layer width	130%					
First layer speed	20%					

extrusion during fabrication of the same specimen, we considered two different orientations:  $0^\circ$  ( $2 \times 1 \times 1 \text{ cm}^3$ ) and  $90^\circ$  ( $1 \times 1 \times 2 \text{ cm}^3$ ), as presented in Fig. 2. The specimen was printed with CFR-PEEK by varying the layer thickness and printing speed for each orientation during material extrusion. We prepared and modeled the specimen using a computer-aided design (CAD) application, from which an STL file was generated. The file was then read by a slicer

application (Simplify3D) [43] and further processed in the material extrusion machine. A brim was used as a supporting base for the finished product during the deposition of the first layer, as it enhances product quality by minimizing deformation during the printing process [44].

### 2.2.3 Design of experiment (DOE)

We designed our experiment by considering five levels of layer thickness and six levels of printing speed. In this study, the continuous factors are levels of both layer thickness and printing speed. Overall, we performed 30 experiments (five layer thicknesses  $\times$  six printing speeds) in random order to examine the effects on the responses for each orientation of the specimen. We considered a set of responses: build time, filament volume, and EC. Since the time required by the material extrusion machine during the warm-up phase before extrusion was nearly constant throughout the process, variables related to the warm-up phase were not considered as response variables in DOE. Build time as well as filament volume for each part were recorded by the material extrusion machine during the experiments. A power-meter logger, Wattman HPM-100A, was used to measure EC during material extrusion [42]. The response variables are summarized in Table 2.

### 2.2.4 MAR models

MAR can be used to estimate average AM power, similar to the use of MRR in subtractive manufacturing processes. Using the relationship between build time ( $t_b$ ) and filament volume ( $V_f$ ), MAR can be expressed as shown in the following equation:

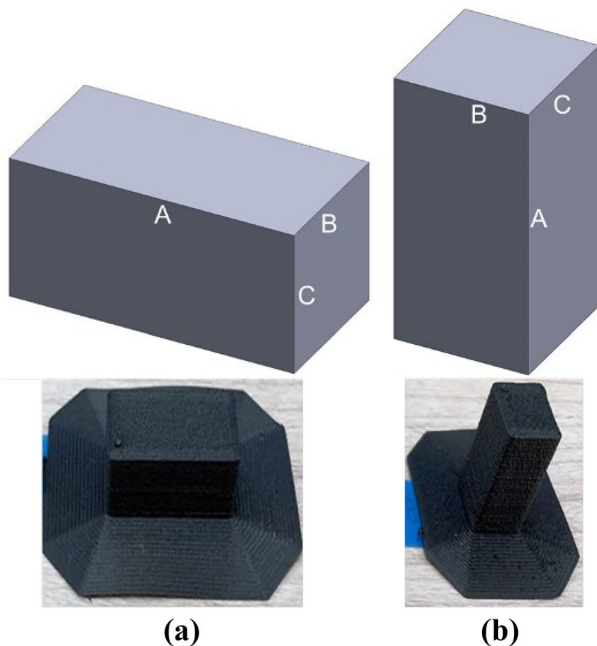


**Fig. 2** A specimen with (a) orientation and (b) orientation and respective brims

**Table 2** Responses examined in the experimental design

Response variable	Description	Unit
Build time	The time required to fabricate a product during building	Seconds
Filament volume	The volume of a finished product including the brim	mm <sup>3</sup>
EC	Energy consumed during heating, building, and cooling	Watt hours

$$MAR = \frac{V_f}{t_b} \tag{1}$$

Also, average build power ( $W_b$ ) can be expressed as a linear function of MAR:

$$W_b = b_0 + b_1 \times MAR \tag{2}$$

In Eq. (2),  $b_0$  and  $b_1$  are constants. The values of these constants were estimated using a regression model based on the experiments in this study, as will be discussed later. Based on 30 sets of experiments with various treatments of layer thickness and printing speed, we measured EC ( $Wh_b$ ) and  $t_b$  during the building state of material extrusion.

Therefore,  $W_b$  can also be calculated using the following equation:

$$W_b = \frac{Wh_b}{t_b} \tag{3}$$

### 2.3 Simulation models of AM power

We propose a method to simulate the power of material extrusion at the facility level. Our proposed method is illustratively summarized in Fig. 3 and described further on what follows.

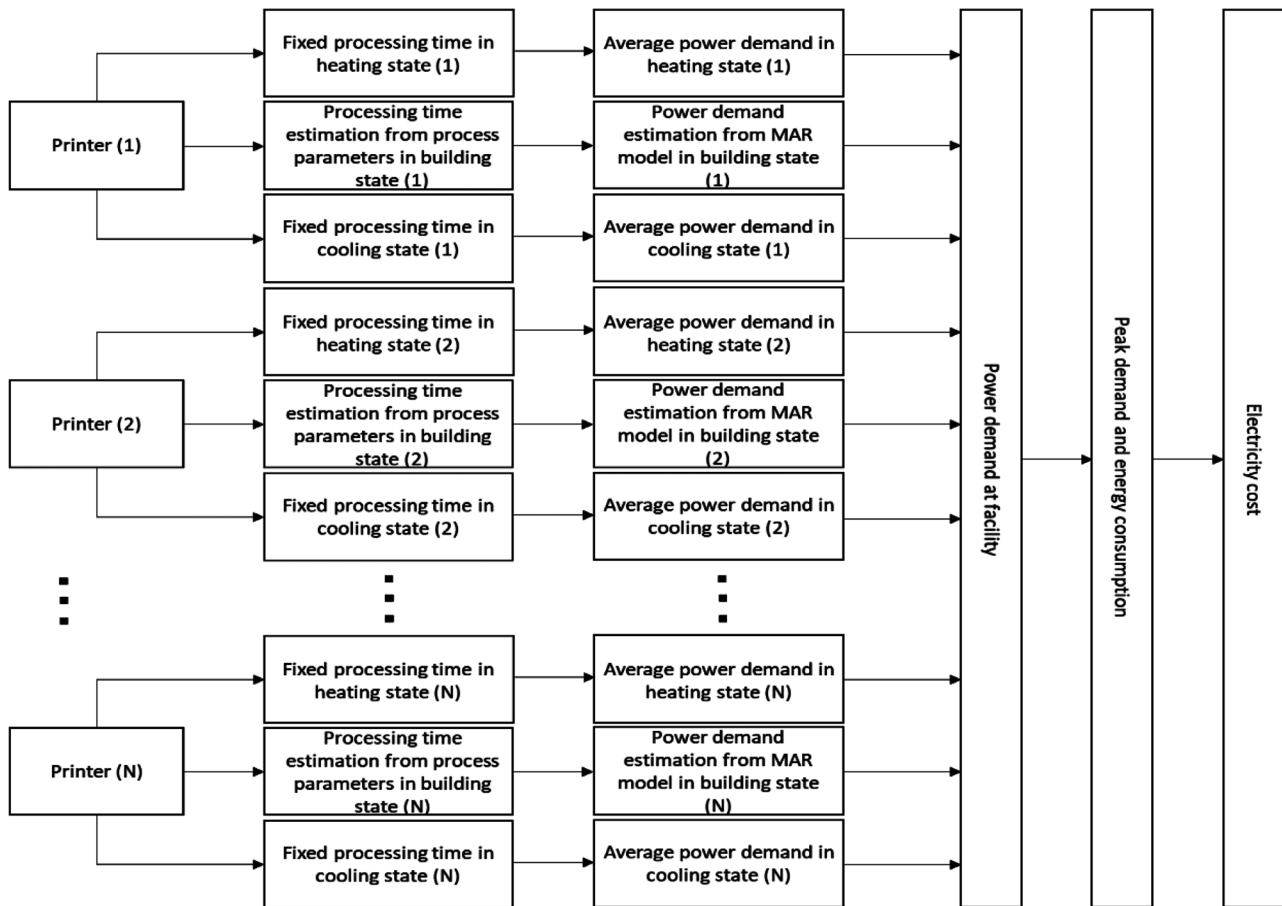


**Fig. 3** Power demand and EC simulation for material extrusion machines using our proposed method



### 2.3.1 Build time estimation model

The build time of material extrusion can be characterized by the amount of time needed by a machine to complete the fabrication of a product [32]. Build time varies with the different process parameters involved in the printing process as well as the geometrical shape and orientation of parts. Acceleration and deceleration of the extruding nozzle and infill percentages are also taken into account by including layer thickness and printing speed as process parameters in the build time estimation model [32, 33]. Table 3 describes the process parameters and their measurement units.

The time required during the extrusion process can be defined as the extrusion time of the material extrusion machine ( $t_{b,ex}$ ). After the completion of one layer, the extruding nozzle moves back to its initial position to start the extrusion for the next layer. During this movement of the nozzle, no extrusion occurs, and the time required for the nozzle movement can be defined as the non-extrusion time of the machine ( $t_{b,nex}$ ). Therefore, total build time ( $t_b$ ) can be represented as follows [32, 33]:

$$t_b = t_{b,ex} + t_{b,nex} \tag{4}$$

The delay time ( $t_{b,d}$ ) during extrusion is included in the build time estimation model to account for the additional time needed for each layer to solidify before depositing the next layer [45]. Hence,  $t_{b,ex}$  is comprised of the time the extruding nozzle moves at constant speed ( $t_{b,c}$ ), the time during the acceleration and deceleration of the extruding nozzle ( $t_{b,a}$ ), the filament retraction time ( $t_{b,r}$ ), and  $t_{b,d}$ . Therefore,  $t_{b,ex}$  can be expressed by the following equation:

$$t_{b,ex} = t_{b,c} + t_{b,a} + t_{b,r} + t_{b,d} = \left( \frac{l_1 \times w_1 \times I_p}{v_{ps,1} \times w_{ex,1}} \times \frac{h_1}{l_{t,1}} + \frac{l_r \times w_r \times I_p}{v_{ps,r} \times w_{ex,r}} \times \frac{h_r}{l_{t,r}} \right) + \frac{v_{ps}}{a_{xy}} + \frac{2 \times l_{fr}}{v_{fr}} + \frac{t_{i,d} \times h_d}{l_{t,d}} \tag{5}$$

where

- $l_1$  = part length for producing the first layer, mm
- $w_1$  = part width for producing the first layer, mm

**Table 3** Process parameters of material extrusion

Parameters	Unit
Layer thickness, $l_t$	mm
Printing speed in XY plane, $v_{ps}$	mm/min
Infill percentage, $I_p$	-
Extruding nozzle repositioning speed in XY plane, $v_{xy}$	mm/min
Acceleration/deceleration in XY plane, $a_{xy}$	mm/min <sup>2</sup>
Filament retraction speed, $v_{fr}$	mm/min

- $h_1$  = part height for producing the first layer, mm
- $I_p$  = infill percentage (%)
- $v_{ps,1}$  = printing speed in XY plane for producing the first layer, mm/min = 20%  $\times v_{ps}$
- $v_{ps}$  = printing speed in XY plane, mm/min
- $w_{ex,1}$  = extrusion width for producing the first layer, mm = 130%  $\times l_{t,1}$
- $l_{t,1}$  = layer thickness for producing the first layer, mm = 0.1 mm
- $l_r$  = part length for producing the remaining layers, mm
- $w_r$  = part width for producing the remaining layers, mm
- $h_r$  = part height for producing the remaining layers, mm
- $v_{ps,r}$  = printing speed in XY plane for producing the remaining layers, mm/min =  $v_{ps}$
- $w_{ex,r}$  = extrusion width for producing the remaining layers, mm
- $l_{t,r}$  = layer thickness for producing the remaining layers, mm
- $a_{xy}$  = acceleration or deceleration in XY plane, mm/min<sup>2</sup>
- $l_{fr}$  = length of the retracted filament, mm
- $v_{fr}$  = filament retraction speed, mm/min
- $t_{i,d}$  = interval between each printing cycle, min
- $l_{t,d}$  = layer thickness of each layer, mm
- $h_d$  = part height without the first layer, mm

The  $w_{ex,1}$  and  $v_{ps,1}$  values are based on the settings of the slicing software (Simplify3D) used to print  $2 \times 1 \times 1 \text{ cm}^3$  and  $1 \times 1 \times 2 \text{ cm}^3$  blocks. The non-extrusion build time ( $t_{b,nex}$ ) consists of two portions: extruding nozzle movement time and extruding nozzle repositioning time in the XY plane [32]. In order to calculate the extruding nozzle movement time in the XY plane during the non-extrusion

process, we calculate the displacement in the X-axis ( $l_{nm,x}$ ) and the Y-axis ( $l_{nm,y}$ ) with the extruding nozzle repositioning speed ( $v_{xy}$ ). For the extruding nozzle repositioning time calculation in the X, Y, and Z directions, we consider  $a_{xy}$  and  $v_{xy}$ . Thus, the equation of  $t_{b,nex}$  is as follows:

$$t_{b,nex} = \frac{l_{nm,x} + l_{nm,y}}{v_{xy}} + \frac{v_{xy}}{a_{xy}}, \tag{6}$$

where

- $l_{nm,x}$  = extruding nozzle displacement in X-axis during the non-extrusion process, mm
- $l_{nm,y}$  = extruding nozzle displacement in Y-axis during the non-extrusion process, mm

$v_{xy}$  = extruding nozzle repositioning speed during the non-extrusion process, mm/min

$a_{xy}$  = extruding nozzle repositioning acceleration during the non-extrusion process, mm/min<sup>2</sup>

Finally,  $t_b$  can be represented as follows:

$$t_b = \frac{l_1 \times w_1 \times I_p}{v_{ps,1} \times w_{ex,1}} \times \frac{h_1}{l_{t,1}} + \frac{l_r \times w_r \times I_p}{v_{ps,r} \times w_{ex,r}} \times \frac{h_r}{l_{t,r}} + \frac{v_{ps}}{a_{xy}} + \frac{2 \times l_{fr}}{v_{fr}} + \frac{t_{i,d} \times h_d}{l_{t,d}} + \frac{l_{nm,x} + l_{nm,y}}{v_{xy}} + \frac{v_{xy}}{a_{xy}} \tag{7}$$

### 2.3.2 Facility level power model

To simulate the facility level power model, we consider a hypothetical AM shop. We define  $W_{i,t}$  as the time series power demand of each material extrusion machine, where  $i$  is the index of the machine and  $t$  is time. Then, the power demand at the facility level can be calculated by accumulating the power demand of each machine in the facility. If  $N$  machines are operating in an AM facility, the facility level power ( $X_t$ ) at  $t$  can be expressed as follows:

$$X_t = \sum_{i=1}^N W_{i,t}, \tag{8}$$

where  $W_{i,t}$  = time series power demand of material extrusion machine  $i$  at time  $t$ .

Figure 4 shows an example power profile of two parallel material extrusion machines.

We developed and applied a DES model in this study to account for multiple material extrusion machines. Using the DES model, we considered various simulation configurations. In our study, the model is based on a simple queueing model.

The interarrival time (IAT) of the queueing model is determined with the machine utilization information defined in simulated scenarios. Also, the processing time of the queueing model is based on the average heating time, average build time, and average cooling time from the experiments. IAT and processing time are then defined using various probability distribution functions for the simulation. By using DES, we can obtain the departure time ( $t_d$ ) of each finished product from the material extrusion machine. Then, the power demand at the equipment level and the facility level is calculated by using a numerical simulation approach based on  $t_d$ , which is obtained from DES. During the numerical simulation, the power demand for each machine at a specific time moment is calculated, and the power demand of all machines in the facility can be obtained by calculating the total sum of the power demand of every machine, as shown in Eq. (8). The simulation approach is briefly described in Table 4.

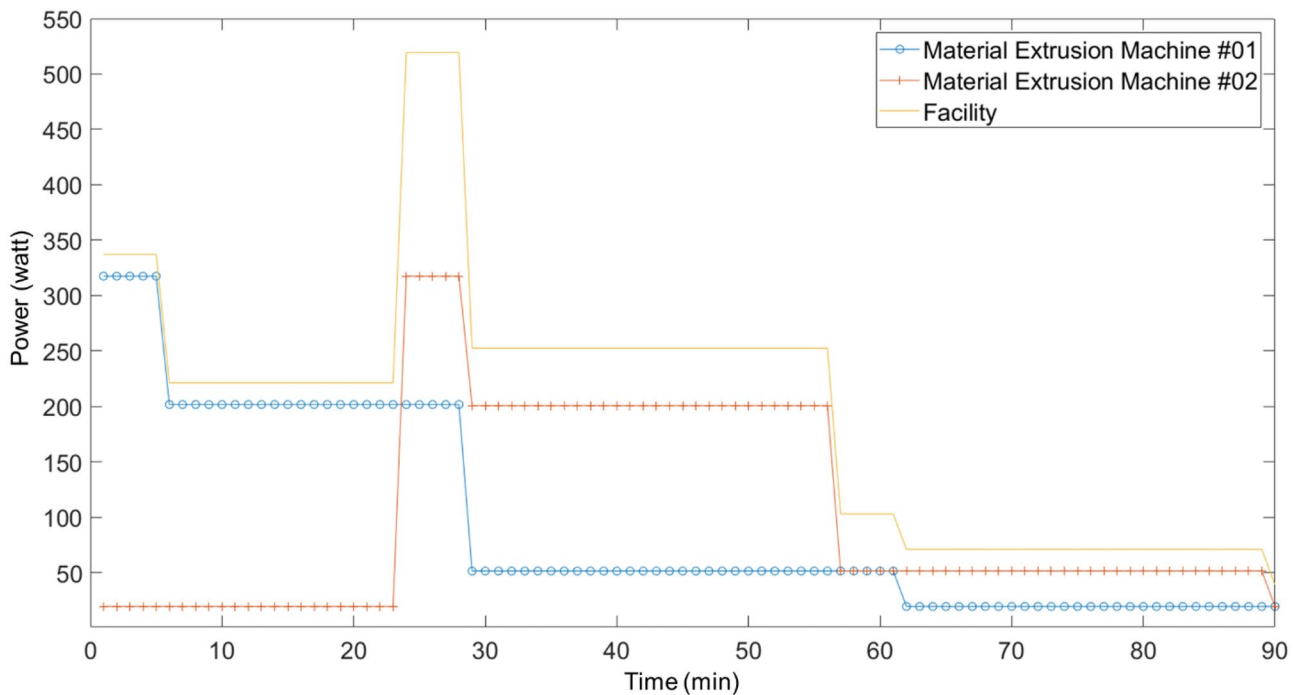


Fig. 4 Power profile example of two material extrusion machines at the equipment level and the facility level

**Table 4** Simulation steps to estimate equipment level and facility level power demand

Step no.	Simulation type	Description of simulation procedures
1	Discrete event	Develop a discrete event simulation model for a system with parallel material extrusion machines
2	Discrete event	Execute the simulation model of material extrusion machines
3	Discrete event	Gather departure time $t_d$ from each material extrusion machine
4	Numerical	Simulate power demand of each material extrusion machine using the MAR model for each $t_d$
5	Numerical	Simulate facility level power demand by adding all equipment level power demands

## 2.4 Material extrusion machine control strategy

A control strategy can be developed and adopted if one material extrusion status requires more kilowatts than another. For example, we restrict the number of material extrusion machines that can enter the heating state at the same time. This strategy lowers the demand charge at the facility level because the heating state requires more power than the building and cooling states. On one hand, if we make more products in a shorter average cycle time, we are likely to pay higher energy costs due to higher demand charges. On the other hand, if we control the number of machines entering the heating state to keep the demand charge lowered, more raw materials will be waiting, and the average cycle time will become longer. Thus, the throughput will be compromised, leading to greater productivity loss. Then, a trade-off analysis between the average cycle time and energy costs can be conducted using a set of control strategies to limit the number of machines in the heating state.

## 3 Results and discussion

### 3.1 Power models with MAR

We performed an ANOVA analysis on the results obtained from the experiments in our DOE. As discussed earlier, we performed two different sets of experiments for  $0^\circ$  ( $2 \times 1 \times 1 \text{ cm}^3$ ) and  $90^\circ$  ( $1 \times 1 \times 2 \text{ cm}^3$ ) orientations of the specimen to examine energy performances while printing identical specimens. Therefore, the results from both sets of experiments are integrated into a combined regression model that expresses kilowatts as a function of MAR.

Tables 5, 6 and 7 present the values of the intercept and the coefficient of MAR in the individual and combined regression models of average build power ( $W_b$ ) for the  $2 \times 1 \times 1 \text{ cm}^3$  and  $1 \times 1 \times 2 \text{ cm}^3$  blocks. The tables also present the  $p$  values of the  $t$ -statistics and  $R^2$  values for MAR. The  $p$  value

**Table 5** Parameter estimates for the regression model of  $W_b$  for the  $2 \times 1 \times 1 \text{ cm}^3$  block

Term	Estimate	Std. error	$t$ Ratio	$R^2$	$p$ value
Intercept	195.1	1.16	168.02		<0.0001
MAR	6.57	0.90	7.26	0.65	<0.0001

indicates that MAR is statistically significant at a 5% level in both the individual and the combined regression models.

In Fig. 5, MAR is presented on the horizontal axis and  $W_b$  on the vertical axis. The regression equation for estimating  $W_b$  of the  $2 \times 1 \times 1 \text{ cm}^3$  block can be expressed as follows:

$$W_{b,2 \times 1 \times 1} = 195.1 + 6.57MAR \quad (9)$$

where

$W_{b,2 \times 1 \times 1}$  = average build power for printing the  $2 \times 1 \times 1 \text{ cm}^3$  block, watts

MAR = material addition rate for printing the  $2 \times 1 \times 1 \text{ cm}^3$  block,  $\text{mm}^3/\text{s}$

Also, the regression equation for estimating  $W_b$  of the  $1 \times 1 \times 2 \text{ cm}^3$  block can be expressed as follows:

$$W_{b,1 \times 1 \times 2} = 196.4 + 10.24MAR \quad (10)$$

where

$W_{b,1 \times 1 \times 2}$  = average build power for printing the  $1 \times 1 \times 2 \text{ cm}^3$  block, watts

MAR = material addition rate for printing the  $1 \times 1 \times 2 \text{ cm}^3$  block,  $\text{mm}^3/\text{s}$

Finally, a regression equation for the combined model can be expressed as follows:

$$W_{b,combined} = 196.18 + 8.04MAR \quad (11)$$

where

$W_{b,combined}$  = average combined build power, watts

MAR = material addition rate,  $\text{mm}^3/\text{s}$

As shown in Fig. 5, the combined regression line is located between the two regression lines corresponding to the two orientations of the specimen. As discussed, heating and cooling power are stable in the process. Thus, the combined heating power is calculated by considering the average heating power obtained before the material extrusion of the  $2 \times 1 \times 1 \text{ cm}^3$  block and the  $1 \times 1 \times 2 \text{ cm}^3$  block. Combined cooling power is calculated

**Table 6** Parameter estimates for the regression model of  $W_b$  for the  $1 \times 1 \times 2 \text{ cm}^3$  block

Term	Estimate	Std. error	$t$ Ratio	$R^2$	$p$ value
Intercept	196.4	1.87	104.75		<0.0001
MAR	10.24	1.51	6.76	0.68	<0.0001



**Table 7** Parameter estimates for the combined regression model of  $W_b$

Term	Estimate	Std. error	t Ratio	R <sup>2</sup>	p value
Intercept	196.18	1.62	121.24		< 0.0001
MAR	8.04	1.28	6.26	0.40	< 0.0001

by following a similar approach. Hence, the combined heating power ( $W_{h,combined}$ ) and the combined cooling power ( $W_{c,combined}$ ) are  $W_{h,combined} = 319.5W$  and  $W_{c,combined} = 51.5W$ , respectively. These values were obtained when printing CFR-PEEK parts using material extrusion on an Apium P220 machine in accordance with the design specified in this study.

### 3.2 Illustrative examples with simulation models

#### 3.2.1 Estimation of build time

In this section, we discuss the build time estimation model from Subsect. 2.3.1 using a numerical example. We estimated the printing time for our simulation models using  $l_t = 0.1$  mm and  $v_{ps} = 1,500$  mm/min. The build time measured in the experiments was  $t_m = 2,804$  s. Once the values of all the relevant parameters are plugged into Eq. (7), the following estimation can be obtained:

$$\begin{aligned}
 t_b &= \frac{l_1 \times w_1 \times I_p}{v_{ps,1} \times w_{ex,1}} \times \frac{h_1}{l_{t,1}} + \frac{l_r \times w_r \times I_p}{v_{ps,r} \times w_{ex,r}} \times \frac{h_r}{l_{t,r}} + \frac{v_{ps}}{a_{xy}} + \frac{2 \times l_{fr}}{v_{fr}} + \frac{t_{i,d} \times h_d}{l_{i,d}} + \frac{l_{nm,x} + l_{nm,y}}{v_{xy}} + \frac{v_{xy}}{a_{xy}} \\
 &= \frac{20 \times 10 \times 1}{(0.2 \times \frac{1,500}{60}) \times (1.3 \times 0.1)} \times \frac{0.1}{0.1} + \frac{20 \times 10 \times 1}{\frac{1,500}{60} \times 0.48} \times \frac{9.9}{0.1} + \frac{\frac{1,500}{60}}{1,500} \times \frac{10}{0.1} + \frac{2 \times 2}{70} \times \frac{10}{0.1} + \frac{8.1 \times 9.9}{0.1} + \frac{20 + 10.24}{\frac{4,800}{60}} \times \frac{10}{0.1} + \frac{\frac{4,800}{60}}{1,500} \times \frac{10}{0.1} \\
 &= 2,810s
 \end{aligned}$$

The values of most of the above parameters can be obtained directly from the process parameters and printer settings. However, we estimated the values of a few parameters such as  $t_{i,d}$  and  $l_{nm,y}$ . Given a layer thickness of 0.1 mm and a speed of 1,500 mm/min for the  $2 \times 1 \times 1$  cm<sup>3</sup> block, the printing time of each layer was estimated at around 17 s, without considering any interval between two consecutive printing cycles. However, a delay time of about 20 to 30 s would be required for the recently deposited layers to solidify and form an adequate base for the next layer [46]. Therefore, we assumed an interval of around 8 to 10 s between two printing cycles and modified the settings in the slicer software accordingly. Hence, total printing time to complete the deposition of one layer ( $t_{i,d}$ ) with a layer thickness of 0.1 mm and a printing speed of 1,500 mm/min was assumed to be 25 s (= 17 + 8) for this experiment. During material extrusion, sufficient clearance must be maintained between the last deposited layer and the next layer to be deposited. Correspondingly, we adjusted the extruding nozzle displacement setting in the slicer software to prevent overlapping between concurrent printed layers. Thus, we conservatively assumed that value of the extruding nozzle displacement in the Y-axis was the sum of the width of the specimen and half of the extrusion width ( $l_{nm,y} = 10 + \frac{0.48}{2} = 10.24$  mm). Finally, an

**Fig. 5** Estimated average build power from the individual and combined MAR regression models

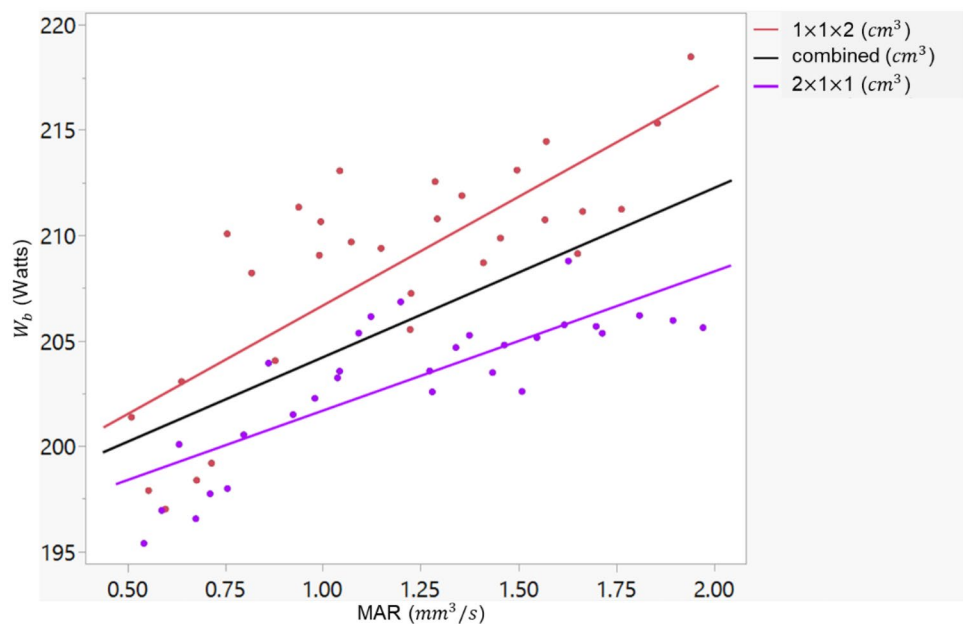


**Table 8** Demand and energy rates in four states of the USA

Demand and energy rate	States			
	NE	MO	HI	WA
\$/kW	19.95	1.71	19.5	4.2
\$/kWh	0.0891	0.0944	0.2617	0.074

error between the build time measured in our experiments ( $t_m$ ) and the build time estimated in our model ( $t_b$ ) was calculated as  $\left| \frac{t_m - t_b}{t_m} \right| = \left| \frac{2,804 - 2,810}{2,804} \right| = 0.22\%$ .

Since there were 30 experimental observations, we were able to compare 30 experimental build times with 30 estimated build times for validation and verification. Overall, the average error rate for the 30 observations was approximately 0.6%. This rate suggests that the build time model provides reliable estimates and can be used for simulations.

### 3.2.2 Electricity rate in US states

In this study, we used the demand rates (\$/kW) and energy rates (\$/kWh) of four different US states, Hawaii (HI), Missouri (MO), Nebraska (NE), and Washington (WA), to obtain more practical results. Information about these rates was collected from [8] and is presented in Table 8.

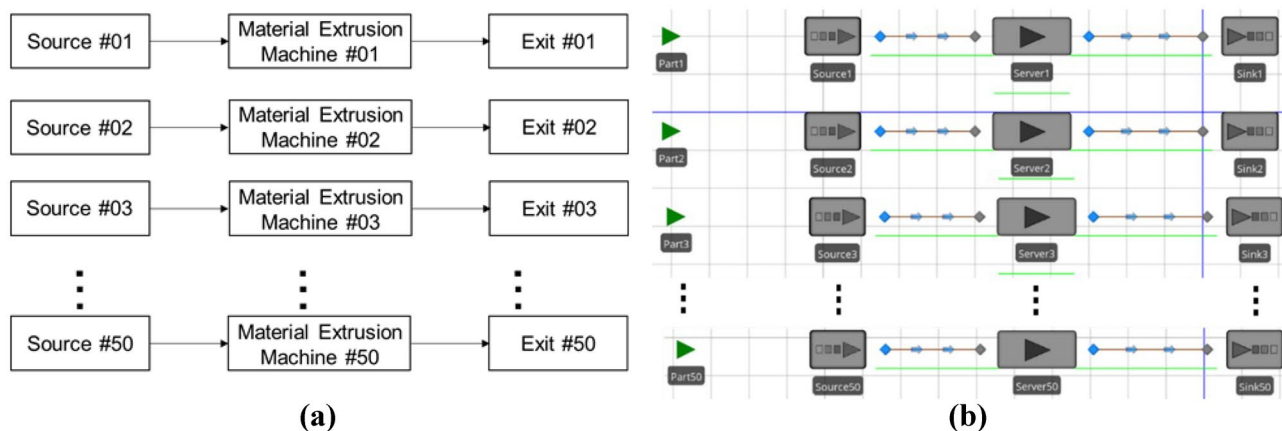
### 3.2.3 Simulation results

A hypothetical AM facility with 50 parallel material extrusion machines for CFR-PEEK was posited for the estimation of power demands and electricity costs. With respect to the product to be made using material extrusion, we considered a  $1 \times 1 \times 1 \text{ cm}^3$  specimen and a  $1.5 \times 1.5 \times 1.5 \text{ cm}^3$  specimen. Geometries of specimens used in the simulation were selected differently from those used in our experiments to demonstrate the applicability of the MAR power model,

thereby applying the model to other cases that are not direct results of the experiments. We assumed that the average IAT of each raw material at the source of each machine follows an Exponential distribution. We also assumed a simulation time of 45,000 min ( $= 45,000 \text{ min} \approx 31 \text{ days} \times 24 \text{ h} \times 60 \text{ min}$ ) to derive the monthly electricity costs. After simulating various sets of configurations, we calculated the peak demand, EC, and monthly utility costs for the hypothetical AM facility. Figure 6 presents the simulation model of the 50 parallel material extrusion machines. More specifically, a simulation case study with 40 scenarios was performed using the DES approach, in which we considered six different sets of process parameters.

Table 9 presents the levels of factors for the sets of material extrusion process parameters considered in the simulation. As seen from the table, build time in the simulation was assumed to follow two probability distributions: normal and exponential. Also, an exponentially distributed waiting time of material extrusion machines was considered in the simulation experiments. Assumptions of probability distributions for build time and average waiting time of material extrusion machines were made according to related simulation studies available [21, 47, 48]. Furthermore, material extrusion machine utilization ( $\rho$ ) in Table 9 is defined as the likelihood of the machine being occupied, or the percentage of time the machine is busy with the fabrication of parts [49]. In other words, machine utilization is the ratio of the average printing time of products to the average IAT of raw materials. Machine utilization is typically used in simulation or queueing studies. Two machine utilization factors (0.4 and 0.8) were considered in this study based on the relevant simulation study [50] as well. The DES results were then used as inputs for a numerical simulation to generate time series power profiles for evaluating performance measures in each scenario.

The results for Set 1, a simulation with a  $1 \times 1 \times 1 \text{ cm}^3$  specimen and normally distributed build time, are presented

**Fig. 6** A conceptual diagram (a) and Simio simulation model (b) for 50 material extrusion machines

**Table 9** Levels of factors considered in the simulation

Parameters	Level 1	Level 2	Level 3
Number of material extrusion machines allowed in the heating state	1	25	50
Material extrusion machine control policy	P <sub>1</sub>	P <sub>25</sub>	P <sub>50</sub>
Material extrusion machine utilization ( $\rho$ )	0.4	0.8	
Specimen size (length $\times$ width $\times$ height, cm <sup>3</sup> )	1 $\times$ 1 $\times$ 1	1.5 $\times$ 1.5 $\times$ 1.5	
Build time probability distribution	Normal	Exponential	
Mean waiting time (WT) of material extrusion machines before entering the heating state (min)	0.17	1	
Distribution of average waiting time of material extrusion machines	Exponential		

in Table 10 by the various process and simulation parameters. The average interarrival time of the raw materials as well as the average heating time, average build time, and average cooling time during material extrusion are denoted as average IAT, average HT, average BT, and average CT, respectively, in the table. Case 1–1 (C1-1) is the baseline scenario for comparing other cases in the table, and each counterpart is different from the baseline in at least one parameter. For each scenario, we controlled the number of machines that entered the heating state (see 2nd column of Table 10). As shown in Table 9, we considered three control strategies in this study, P<sub>1</sub>, P<sub>25</sub>, and P<sub>50</sub>, which allowed one, 25, or 50 machines to enter the heating state at a time, respectively. If a machine cannot enter the heating status due to this control, it waits for a random time (WT) until attempting to enter the heating status again (see 10th column in Table 10). For the top five cases in Set 1, the control strategies of material extrusion machines and the mean WT varied by the levels shown in Table 9. For the bottom five cases in Set 1, the parameters changed similarly while  $\rho$  (machine utilization) increased from 0.4 (C1-1) to 0.8.

The number of printed parts, number of waiting raw materials, and average cycle time are obtained from the simulation results. Average cycle time is defined as the average amount of time that it takes to finish printing one complete part, including the waiting time. Peak kilowatt is equal to the maximum kilowatt value obtained in the heating, building, and cooling states during 45,000 min of material extrusion operations. Total kilowatt hour is calculated by multiplying the average kilowatt and the total simulation time (=45,000 min). Furthermore, electricity costs are calculated by adding the demand charge (= peak demand  $\times$  demand rate) and the energy charge (= energy usage  $\times$  energy rate).

For C1-1, peak kilowatt and total kilowatt hour were relatively low since control strategy P<sub>1</sub> was adopted. Also, the average cycle time increased in C1-1. Hence, productivity was relatively low due to the increase in unprocessed raw materials in the production process over time. Compared with results of C1-1, peak kW, total kWh, electricity costs, and throughputs rose considerably in C1-2 due to more material extrusion machines being allowed to heat with P<sub>25</sub>. Also,

the average cycle time decreased rapidly in C1-2 because more machines could process parts. A negligible change in performance measures is observed between C1-1 and C1-3 due to similarities in the simulation parameters. Compared with C1-1, performance measures significantly increased with P<sub>25</sub> in C1-4. It can also be noted that an increase in the average WT had a minor effect on performance measures. Compared to C1-1, C1-5 exhibited a rising trend in performance measures as well. In this case, the change in peak kW was relatively higher since P<sub>50</sub> was employed. For C1-6, the arrival rate of raw materials increased with  $\rho$ , and thus, the number of waiting raw materials in C1-6 rose much higher with a longer average cycle time compared to C1-1. Accordingly, productivity in C1-6 showed a considerable drop. A similar result is found in a comparison between C1-1 and C1-8. Compared to C1-1, C1-7 showed a significant increase in performance measures with notable reductions in average cycle time as more raw materials were processed with P<sub>25</sub>. A similar observation can be made in comparisons between C1-1 and C1-9 and between C1-1 and C1-10. In terms of electricity costs in the four US states, relatively higher electricity costs were observed in HI since \$/kW and \$/kWh are greater there than in the other three states. Also, WA demonstrated the lowest utility costs among the four states because \$/kW and \$/kWh are relatively low.

While  $\rho$  increased from 0.4 to 0.8 in 10 cases of Set 1, we observe similar peak kilowatts in the respective counterpart scenarios. This similarity can be explained by the number of machines allowed to be working at a time. Since the control strategy for material extrusion machines remained the same for higher  $\rho$ , the increase in the number of raw materials and in productivity due to higher  $\rho$  was constrained by the same number of machines available for the heating status. Hence, peak kilowatt did not show any noticeable change in scenarios of Set 1 with an increase in  $\rho$ .

As seen from the simulation results, the number of waiting raw materials is similar in C1-4 (5) and C1-5 (5). We observe similar findings in C1-9 (84) and C1-10 (92) as well. Thus, the number of printed parts in C1-4 and C1-5 scenarios as well as in C1-9 and C1-10 scenarios is expected to be similar in our simulation study. It is noticed that 84

**Table 10** Results with a  $1 \times 1 \times 1 \text{ cm}^3$  specimen and Normally distributed build time (Set 1)

Case no	No. of material extrusion machine in heating state	Material extrusion machine control policy	Avg. IAT (min)	$\rho$	Avg. BT (min)	Std. of BT (min)	BT dist	Sum of avg. HT, BT, and CT (min)	Avg. WT (min)	WT dist	Volume ( $\text{cm}^3$ )	No. of printed parts	No. of waiting raw materials	Avg. cycle time (min)	Peak kW	Total kWh	Electricity cost (\$)			
																	NE	MO	HI	WA
C1-1	1	P <sub>1</sub>	147	0.4	21.2	5.3	Norm	58.9	0.17	Exp	1	9,717	5,751	8,323	2.9	1,754	214	171	516	142
C1-2	25	P <sub>25</sub>	147	0.4	21.2	5.3	Norm	58.9	0.17	Exp	1	15,487	4	78	13	2,364	470	245	872	230
C1-3	1	P <sub>1</sub>	147	0.4	21.2	5.3	Norm	58.9	1	Exp	1	9,673	5,690	8,420	2.9	1,751	214	170	515	142
C1-4	25	P <sub>25</sub>	147	0.4	21.2	5.3	Norm	58.9	1	Exp	1	15,583	5	79	13	2,372	471	246	875	230
C1-5	50	P <sub>50</sub>	147	0.4	21.2	5.3	Norm	58.9	-	Exp	1	15,499	5	78	15.9	2,363	527	250	928	242
C1-6	1	P <sub>1</sub>	74	0.8	21.2	5.3	Norm	58.9	0.17	Exp	1	9,719	20,858	15,321	2.9	1,753	214	170	515	142
C1-7	25	P <sub>25</sub>	74	0.8	21.2	5.3	Norm	58.9	0.17	Exp	1	30,913	90	174	13	3,987	615	399	1,297	350
C1-8	1	P <sub>1</sub>	74	0.8	21.2	5.3	Norm	58.9	1	Exp	1	9,672	21,094	15,523	3	1,752	216	171	517	142
C1-9	25	P <sub>25</sub>	74	0.8	21.2	5.3	Norm	58.9	1	Exp	1	30,639	84	175	13	3,961	613	396	1,290	348
C1-10	50	P <sub>50</sub>	74	0.8	21.2	5.3	Norm	58.9	-	Exp	1	30,604	92	176	15.9	3,950	669	400	1,343	359

additional parts are fabricated in C1-4 (15,583) compared to C1-5 (15,499), while C1-9 (30,639 parts) has 35 more printed parts in comparison to C1-10 (30,604 parts). A slight variation in productivity appears to be the result of random effects during simulation. Also, differences between throughputs in C1-4 and C1-5 as well as in C1-9 and C1-10 are 0.54% and 0.11%, respectively. This suggests that the differences are insignificant with respect to the total number of parts printed in the corresponding scenarios.

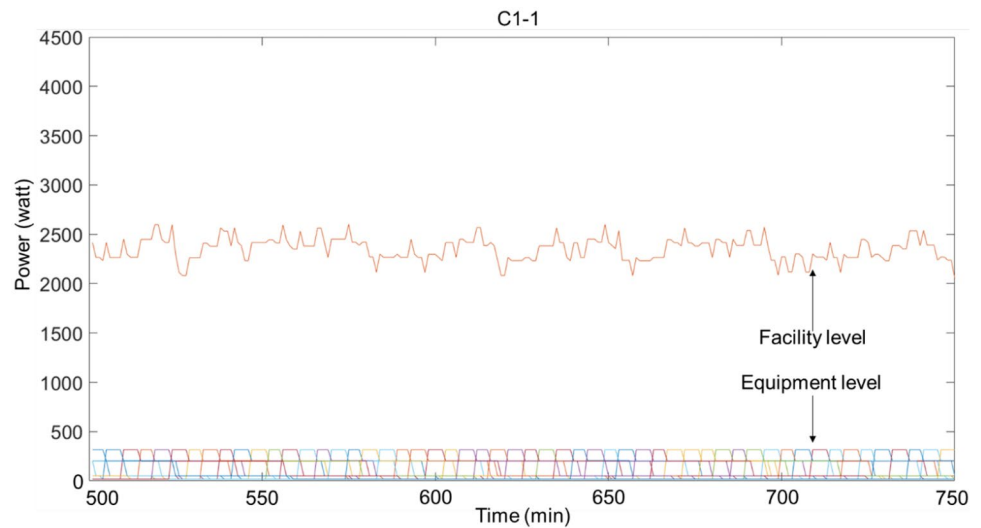
The power profiles of the 50 material extrusion machines at both the equipment and facility levels for C1-1, C1-2, and C1-5 are presented in Figs. 7, 8 and 9, respectively. These figures show that the facility level power demands of C1-2 and C1-5 were noticeably higher compared to those of C1-1 because more machines were allowed to work at the same time. It can also be noticed that the average power required to print parts is similar for C1-2 and C1-5. The difference between facility level power demands of C1-2 and C1-5 can be well understood with the total number of parts printed during material extrusion. As observed from Table 10, differences between the number of parts fabricated in C1-2 (15,487) and C1-5 (15,499) are small in this study. Hence, the facility level power demands in C1-2 and C1-5 differ by a small amount. For the equipment level, the power profile for each of the 50 machines considered in the simulation experiment is displayed in a different color.

Table 11 shows the results of the 10 scenarios in Set 2, a simulation with a larger product volume ( $1.5 \times 1.5 \times 1.5 \text{ cm}^3$ ). In Table 11, no major increase in throughputs, average cycle time, or total kilowatt hour is observed from C2-1 to C2-5. Comparisons between C2-1 and C2-6, C2-1 and C2-7, and so on reveal a trend similar to that found in Set 1. The results of peak kW from C2-1 to C2-10 show a similar pattern to those of Set 1 as well.

The volume of the printed parts in Set 2 was about 3.4 times higher than that of Set 1. Since the volume of the printed parts was larger, it took longer to finish each part. Thus, total kilowatt hour values were relatively higher in Set 2 than those in Set 1 in a comparison between respective counterparts. Also, throughputs in Set 2 were lower compared to those in Set 1 due to an increase in average cycle time. When we conduct a pairwise comparison of peak kilowatt values from the scenarios of Set 2 with those of Set 1, the peak kilowatt values in C2-1, C2-3, C2-6, and C2-8 were greater than those in C1-1, C1-3, C1-6, and C1-8. This difference occurred because more raw materials were being processed in Set 2 at the same time when compared to Set 1. Also, electricity costs were notably higher in Set 2 compared to Set 1 due to higher total kilowatt hour values.

In Table 12, we show the performance measures in 10 cases of Set 3 with a similar configuration to Set 1 and an exponentially distributed build time. Peak kW in most of the scenarios of Set 3, however, was relatively higher than those

**Fig. 7** Power profiles for 50 material extrusion machines at equipment level and facility level for C1-1 with  $P_1$



of Set 1. This difference can be explained by the variability in Exponential versus Normal distributions. The coefficient of variation is 0.25 ( $CV = \text{standard deviation}/\text{mean} = 5.3/21.2$ ) in a normally distributed build time, as in Set 1. CV, however, is 1 in an Exponential distribution. Because build time was exponentially distributed for Set 3, a larger variability in build time distributions could be expected during the simulation. Thus, more variability in build time likely contributed to a higher peak kilowatt in Set 3.

In a comparison of total kilowatt hour between scenarios in Set 1 and Set 3, little change in total kilowatt hour is observed. Similar findings can be observed for the average cycle time as well. Variability in build time distributions in Set 3 would have less impact on average total power compared to peak kilowatt. Thus, total kilowatt hour in Set 3 and Set 1 showed similar results since the total kilowatt hour is calculated by multiplying average kilowatt and total simulation time. Overall, monthly electricity costs were slightly higher in Set 3 compared to Set 1 due to a moderate rise in peak kilowatt while total kilowatt hour values barely changed.

Table 13 presents the results for Set 4, the latter of which was similar to Set 2 except it used an exponentially distributed build time. The performance measures in 10 cases of Set 4 behaved similarly to those in Set 2 when compared to Set 1. Peak kilowatt values in most of the scenarios of Set 4, however, were relatively higher due to the larger variability in the exponentially distributed build time as well as a larger volume of printed parts. Also, the average cycle time and total kilowatt hour in scenarios of Set 4 were similar to those found in Set 2. Utility costs, however, were reasonably higher due to larger peak kilowatt.

Table 14 presents the ratios of various performance measures between the scenarios in Set 1 and the corresponding scenarios in the other three sets. The ratio of each row is

calculated based on two counterpart values in two of the tables.

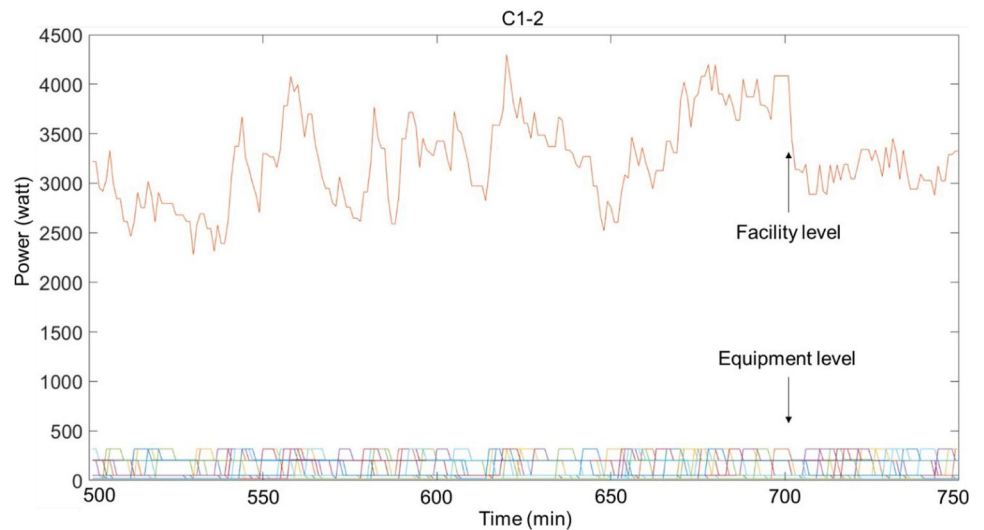
In a comparison between Set 2 and Set 1, differences in the volume of parts had a significant impact on throughputs and average cycle time and a moderate impact on peak kilowatt, total kilowatt hour, and electricity costs. In a comparison between Set 3 and Set 1, the difference between exponential and normal distributions was a major factor for the peak kilowatt and electricity costs because an exponential distribution has higher variability ( $CV = 1$ ) than a normal distribution ( $CV < 1$ ) in our simulation. We can see that most ratios in the peak kilowatt and electricity costs between Set 3 and Set 1 are close to or greater than 1. It seems that some randomness affected the results with ratios less than 1, but these ratios are still close to 1 with a minimum of 0.97 (C3-4/C1-4). Similar conclusions can be drawn when Set 4 is compared to Set 1. The effects on peak kilowatt and utility costs, however, were relatively higher in the ratios between Set 4 and Set 1 compared to the ratios between Set 2 and Set 1 due to more variability with longer printing time.

### 3.2.4 Validation of simulation models

In this subsection, we discuss and show how we validated our simulation model. Simulated average power at the equipment level was compared and validated with the average power of the machine obtained in experiments. For example, the average power measured in the experiment was approximately 127 W for printing a  $2 \times 1 \times 1 \text{ cm}^3$  block with a processing time of 1 h. From our simulated results, the average power of a single machine (Machine #01) was estimated as about 130 W for 1 h of operation of the machine during fabricating a  $2 \times 1 \times 1 \text{ cm}^3$  block. It can be seen that variation in average power at the equipment level during experiments (127 W) and simulations



**Fig. 8** Power profiles for 50 material extrusion machines at equipment level and facility level for C1-2 with  $P_{25}$



(130 W) is 2% approximately. This percentage suggests that our simulation model provides relatively accurate results in the context of the average power and EC at the equipment level. Moreover, we thoroughly examined and validated the facility level power in this simulation study. For example, at the 15th minute of the simulation, the equipment level powers of 50 machines were observed as 205 W (Machine #01), 202 W (Machine #02), and so on for C1-5. Facility level power at the 15th minute was then calculated as 9,997 W by manually adding the equipment level power of 50 machines. The simulated power at the facility level at the 15th minute of the simulation was also obtained as 9,997 W from our simulation model. By following the same approach, we comprehensively validated and verified the facility level power with the results that we manually calculated from the equipment level power for 100 time points of each of the 40 simulation scenarios without any discrepancy. Thus, we believe that our simulation model is valid, and this model

can provide reliable results while calculating the energy performances of AM machines.

### 3.2.5 Trade-offs between average cycle time and energy costs

To show the trade-off between average cycle time and energy costs of material extrusion, an example calculation for evaluating the energy cost of C1-1 is presented first. For this example analysis, we picked the relatively higher demand rate (\$19.95/kW) and relatively lower energy rate (\$0.0891/kWh) of the US state NE. This selection can help us better understand the trade-offs among performance measures in some example scenarios. The total energy cost for C1-1 was calculated as  $Peakdemand \times Demandrate + Energyconsumption \times Energyrate = 2.9 \times 19.95 + 1,754 \times 0.0891 = \$214$ . The average cycle time of C1-1, or 8,323 min, was obtained from the simulation experiment.

**Fig. 9** Power profiles for 50 material extrusion machines at equipment level and facility level for C1-5 with  $P_{50}$

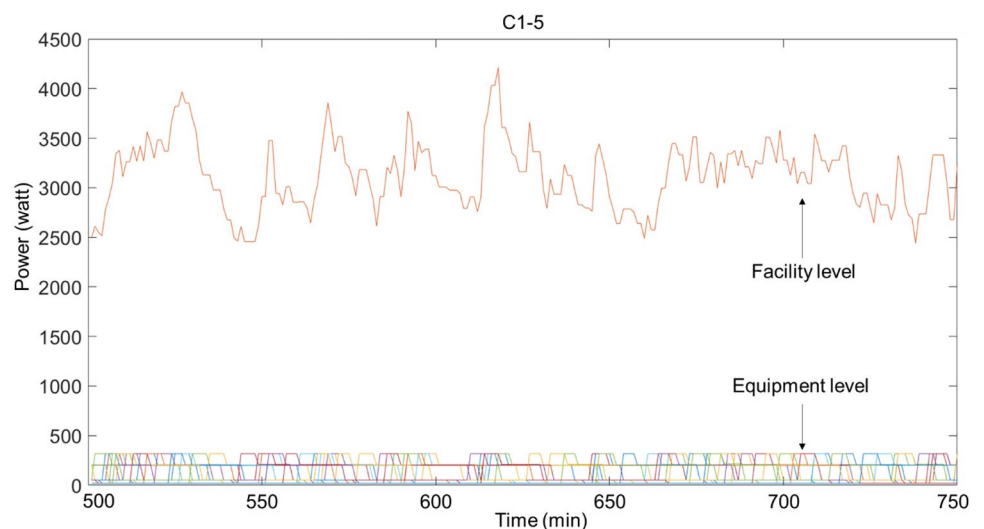


**Table 11** Results with a  $1.5 \times 1.5 \times 1.5 \text{ cm}^3$  specimen and Normally distributed build time (Set 2)

Case no	No. of material extrusion machine control in heating state	Material extrusion machine	Avg. IAT (min)	$\rho$	Avg. BT (min)	Std. of BT (min)	BT dist	Sum of avg. HT, BT, and CT (min)	Avg. WT (min)	WT dist	Volume ( $\text{cm}^3$ )	No. of printed parts	No. of waiting raw materials	Avg. cycle time (min)	Peak kW	Total kWh	Electricity cost (\$)			
																	NE	MO	HI	WA
C2-1	1	P <sub>1</sub>	274	0.4	69	17	Norm	110	0.17	Exp	3.4	8,365	7	173	5.1	2,852	355	278	845	232
C2-2	25	P <sub>25</sub>	274	0.4	69	17	Norm	110	0.17	Exp	3.4	8,072	8	146	13.1	2,775	509	284	982	260
C2-3	1	P <sub>1</sub>	274	0.4	69	17	Norm	110	1	Exp	3.4	8,355	11	181	4.9	2,850	351	277	841	231
C2-4	25	P <sub>25</sub>	274	0.4	69	17	Norm	110	1	Exp	3.4	8,199	6	146	13.1	2,799	511	287	988	262
C2-5	50	P <sub>50</sub>	274	0.4	69	17	Norm	110	-	Exp	3.4	8,262	8	147	16.1	2,820	572	294	1,052	276
C2-6	1	P <sub>1</sub>	137	0.8	69	17	Norm	110	0.17	Exp	3.4	9,566	6,724	9,479	5.2	3,164	386	308	930	256
C2-7	25	P <sub>25</sub>	137	0.8	69	17	Norm	110	0.17	Exp	3.4	16,413	82	322	13.1	4,892	697	484	1,536	417
C2-8	1	P <sub>1</sub>	137	0.8	69	17	Norm	110	1	Exp	3.4	9,504	6,854	9,651	5.2	3,134	383	305	921	254
C2-9	25	P <sub>25</sub>	137	0.8	69	17	Norm	110	1	Exp	3.4	16,540	83	328	13.1	4,920	700	487	1,543	419
C2-10	50	P <sub>50</sub>	137	0.8	69	17	Norm	110	-	Exp	3.4	16,545	82	322	16.1	4,921	759	492	1,601	432

**Table 12** Results with a  $1 \times 1 \times 1 \text{ cm}^3$  specimen and Exponentially distributed build time (Set 3)

Case no	No. of material extrusion machine control in heating state	Material extrusion machine	Avg. IAT (min)	$\rho$	Avg. BT (min)	BT dist	Sum of avg. HT, BT, and CT (min)	Avg. WT (min)	WT dist	Volume ( $\text{cm}^3$ )	No. of printed parts	No. of waiting raw materials	Avg. cycle time (min)	Peak kW	Total kWh	Electricity cost (\$)			
																NE	MO	HI	WA
C3-1	1	P <sub>1</sub>	147	0.4	21.2	Exp	58.9	0.17	Exp	1	9,719	5,761	8,269	4.5	1,746	244	172	544	148
C3-2	25	P <sub>25</sub>	147	0.4	21.2	Exp	58.9	0.17	Exp	1	15,190	8	81	13.1	2,333	469	243	866	228
C3-3	1	P <sub>1</sub>	147	0.4	21.2	Exp	58.9	1	Exp	1	9,674	5,609	8,322	3.7	1,765	232	173	535	146
C3-4	25	P <sub>25</sub>	147	0.4	21.2	Exp	58.9	1	Exp	1	15,088	11	81	12.6	2,320	459	241	853	225
C3-5	50	P <sub>50</sub>	147	0.4	21.2	Exp	58.9	-	Exp	1	15,300	2	81	31.3	2,352	834	276	1,226	306
C3-6	1	P <sub>1</sub>	74	0.8	21.2	Exp	58.9	0.17	Exp	1	9,717	20,988	15,371	5.1	1,766	259	175	561	152
C3-7	25	P <sub>25</sub>	74	0.8	21.2	Exp	58.9	0.17	Exp	1	30,947	64	188	13.2	3,990	619	399	1,302	351
C3-8	1	P <sub>1</sub>	74	0.8	21.2	Exp	58.9	1	Exp	1	9,673	21,236	15,432	4.9	1,752	254	174	555	150
C3-9	25	P <sub>25</sub>	74	0.8	21.2	Exp	58.9	1	Exp	1	30,448	99	187	12.6	3,913	601	391	1,270	343
C3-10	50	P <sub>50</sub>	74	0.8	21.2	Exp	58.9	-	Exp	1	30,555	71	190	47.4	3,955	1,298	454	1,960	492

**Table 13** Results with a  $1.5 \times 1.5 \times 1.5$  cm<sup>3</sup> specimen and Exponentially distributed build time (Set 4)

Case no	No. of material extrusion machine control in heating state	Material extrusion machine control in heating policy	Avg. IAT (min)	$\rho$	Avg. BT (min)	BT dist	Sum of avg. HT, BT, and CT (min)	Avg. WT (min)	WT dist	Volume (cm <sup>3</sup> )	No. of printed parts	No. of waiting raw materials	Avg. cycle time (min)	Peak kW	Total kWh	Electricity cost (\$)			
																NE	MO	HI	WA
C4-1	1	P <sub>1</sub>	274	0.4	69	Exp	110	0.17	Exp	3.4	8,336	16	187	12.4	2,849	501	290	988	263
C4-2	25	P <sub>25</sub>	274	0.4	69	Exp	110	0.17	Exp	3.4	8,204	11	158	15.6	2,813	562	292	1,041	274
C4-3	1	P <sub>1</sub>	274	0.4	69	Exp	110	1	Exp	3.4	8,277	32	195	6.7	2,838	387	279	874	238
C4-4	25	P <sub>25</sub>	274	0.4	69	Exp	110	1	Exp	3.4	8,122	12	160	13.2	2,779	512	285	985	261
C4-5	50	P <sub>50</sub>	274	0.4	69	Exp	110	-	Exp	3.4	8,122	11	159	38.8	2,788	1,023	330	1,487	369
C4-6	1	P <sub>1</sub>	137	0.8	69	Exp	110	0.17	Exp	3.4	9,566	6,854	9,460	8.1	3,118	439	308	973	265
C4-7	25	P <sub>25</sub>	137	0.8	69	Exp	110	0.17	Exp	3.4	16,429	101	397	13.3	4,939	705	489	1,552	421
C4-8	1	P <sub>1</sub>	137	0.8	69	Exp	110	1	Exp	3.4	9,504	6,965	9,623	7.5	3,154	431	311	972	265
C4-9	25	P <sub>25</sub>	137	0.8	69	Exp	110	1	Exp	3.4	16,254	90	385	13.2	4,868	698	482	1,532	416
C4-10	50	P <sub>50</sub>	137	0.8	69	Exp	110	-	Exp	3.4	16,367	65	403	62.4	4,891	1,681	568	2,497	624

Figures 10 and 11 present the trade-off between average cycle time and energy costs for Set 1 and Set 2, respectively, as obtained from the simulation experiments. The X-axis shows the average cycle time and the Y-axis shows energy costs. In both figures,  $\rho = 0.8$  demonstrates relatively higher energy costs than  $\rho = 0.4$ .

As shown in Fig. 10, trade-offs between the average cycle time and energy costs for scenarios in Set 1 with  $\rho = 0.4$  can be analyzed in two groups. One group (G<sub>1</sub>) consists of C1-2, C1-4, and C1-5, and the other group (G<sub>2</sub>), of C1-1 and C1-3. If the priority of a manufacturer is to minimize the average cycle time, G<sub>1</sub> should be considered. For example, manufacturers would be more interested in C1-2 and C1-5 in G<sub>1</sub>, because the average cycle time is considerably lower (78 min) with P<sub>25</sub> and P<sub>50</sub>, respectively. In a comparison between C1-2 (\$470) and C1-5 (\$527), C1-2 would provide more energy cost savings because a reasonable number of material extrusion machines work with P<sub>25</sub>.

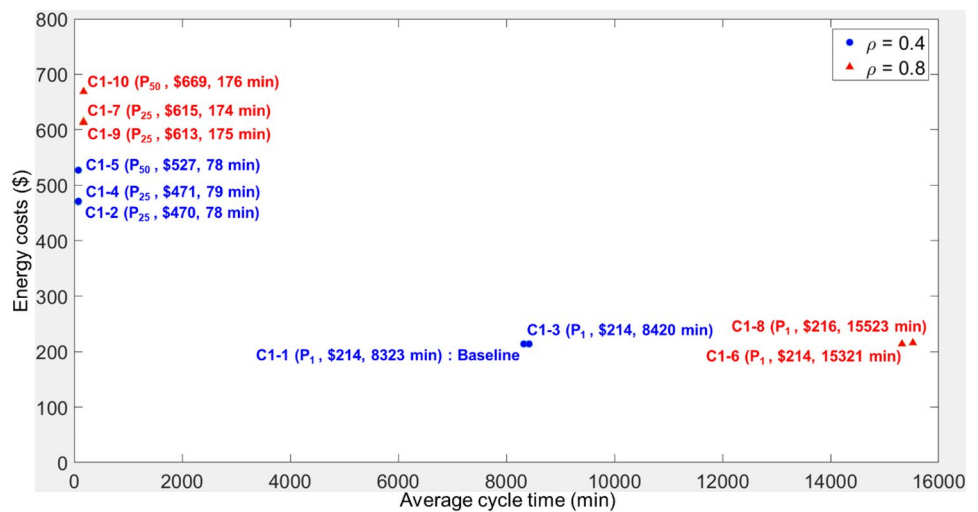
Alternately, if a manufacturer places more emphasis on minimizing energy costs, G<sub>2</sub> would be a better option, because fewer working machines in P<sub>1</sub> result in smaller energy costs for C1-1 and C1-3. Between C1-1 and C1-3, manufacturers would prefer C1-1 (\$214) over C1-3 (\$214), as the average cycle time of C1-1 (8,323 min) is less than that of C1-3 (8,420 min) due to the lower average WT in C1-1. Also, if manufacturers have no preference between minimum average cycle time and minimum energy cost, they can choose P<sub>25</sub> as this policy offers a balanced combination of energy cost and average cycle time, as shown in C1-2 (\$470, 78 min) and C1-4 (\$471, 79 min). For example, average cycle time decreases by more than 8,200 min from C1-1 (P<sub>1</sub>: 8,323 min) to C1-2 (P<sub>25</sub>: 78 min), while energy costs increase only about \$256 from C1-1 (P<sub>1</sub>: \$214) to C1-2 (P<sub>25</sub>: \$470). Thus, if a balanced result is preferred, P<sub>25</sub> would be a better policy than P<sub>1</sub> and P<sub>50</sub> since it can provide a more moderate result. Similar observations can be made for  $\rho = 0.8$  as well, although overall energy costs are relatively higher compared to  $\rho = 0.4$ .

Figure 11 shows that scenarios in Set 2 (C2-1 to C2-5) for  $\rho = 0.4$  should be arranged in one group. In this group, C2-1 (\$355, 173 min) and C2-3 (\$351, 181 min) with P<sub>1</sub> can provide the preferable energy costs and average cycle times because these two scenarios are located at the left-most bottom of the figure. There is a negligible amount of unprocessed raw materials with a lower average cycle time for  $\rho = 0.4$  in C2-1 (7) and C2-3 (11). Thus, more energy cost savings are obtained with less peak demand and less EC with P<sub>1</sub> (C2-1 and C2-3). Between C2-1 and C2-3, manufacturers can pick C2-3 (\$351) over C2-1 (\$355) if they prefer the minimum energy cost. Otherwise, they can select C2-1 to obtain the minimum average cycle time as the average WT of C2-1 (0.17 min) is less than that of C2-3 (1 min). For  $\rho$

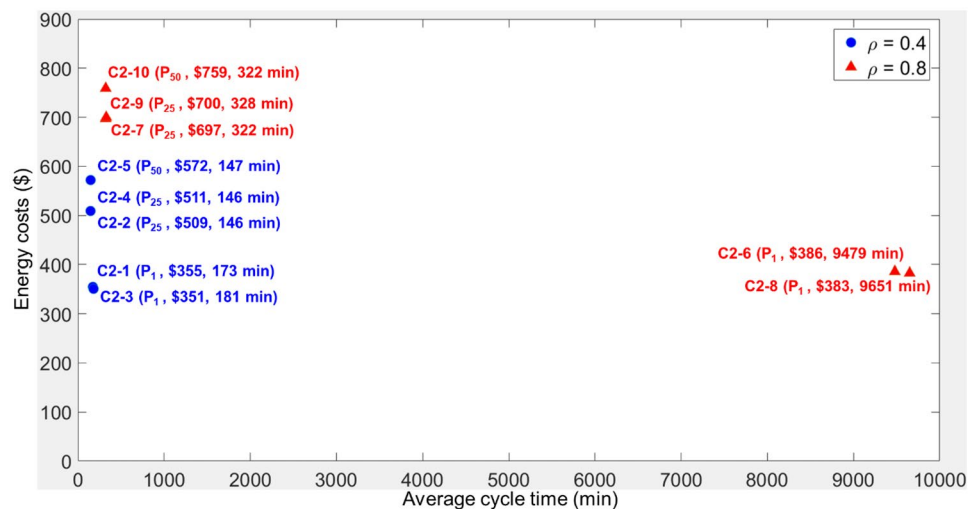
**Table 14** Comparison of results for Case 1–1 through Case 1–10

Cases	No. of printed parts	Average cycle time (min)	Peak kW	Total kWh	Electricity cost (\$)			
					NE	MO	HI	WA
C2-1/C1-1	0.86	0.02	1.75	1.63	1.66	1.63	1.64	1.64
C2-2/C1-2	0.52	1.87	1.01	1.17	1.08	1.16	1.13	1.13
C2-3/C1-3	0.86	0.02	1.68	1.63	1.64	1.63	1.63	1.63
C2-4/C1-4	0.53	1.85	1.01	1.18	1.09	1.16	1.13	1.14
C2-5/C1-5	0.53	1.88	1.01	1.19	1.08	1.17	1.13	1.14
C2-6/C1-6	0.98	0.62	1.80	1.80	1.80	1.80	1.80	1.80
C2-7/C1-7	0.53	1.85	1.01	1.23	1.13	1.21	1.18	1.19
C2-8/C1-8	0.98	0.62	1.72	1.79	1.77	1.79	1.78	1.78
C2-9/C1-9	0.54	1.87	1.01	1.24	1.14	1.23	1.20	1.21
C2-10/C1-10	0.54	1.83	1.01	1.25	1.14	1.23	1.19	1.20
C3-1/C1-1	1.00	0.99	1.54	1.00	1.14	1.01	1.05	1.04
C3-2/C1-2	0.98	1.04	1.01	0.99	1.00	0.99	0.99	0.99
C3-3/C1-3	1.00	0.99	1.29	1.01	1.08	1.02	1.04	1.03
C3-4/C1-4	0.97	1.03	0.97	0.98	0.97	0.98	0.98	0.98
C3-5/C1-5	0.99	1.04	1.97	1.00	1.58	1.10	1.32	1.27
C3-6/C1-6	1.00	1.00	1.76	1.01	1.21	1.03	1.09	1.07
C3-7/C1-7	1.00	1.08	1.02	1.00	1.01	1.00	1.00	1.00
C3-8/C1-8	1.00	0.99	1.63	1.00	1.18	1.02	1.07	1.06
C3-9/C1-9	0.99	1.07	0.97	0.99	0.98	0.99	0.98	0.99
C3-10/C1-10	1.00	1.08	2.99	1.00	1.94	1.14	1.46	1.37
C4-1/C1-1	0.86	0.02	4.28	1.62	2.34	1.70	1.92	1.85
C4-2/C1-2	0.53	2.03	1.20	1.19	1.20	1.19	1.19	1.19
C4-3/C1-3	0.86	0.02	2.32	1.62	1.81	1.64	1.70	1.68
C4-4/C1-4	0.52	2.03	1.02	1.17	1.09	1.16	1.13	1.13
C4-5/C1-5	0.52	2.04	2.45	1.18	1.94	1.32	1.60	1.53
C4-6/C1-6	0.98	0.62	2.78	1.78	2.05	1.81	1.89	1.86
C4-7/C1-7	0.53	2.28	1.02	1.24	1.15	1.23	1.20	1.20
C4-8/C1-8	0.98	0.62	2.49	1.80	1.99	1.82	1.88	1.86
C4-9/C1-9	0.53	2.20	1.02	1.23	1.14	1.22	1.19	1.20
C4-10/C1-10	0.53	2.29	3.93	1.24	2.51	1.42	1.86	1.74

**Fig. 10** Trade-off between average cycle time and energy costs for scenarios in Set 1



**Fig. 11** Trade-off between average cycle time and energy costs for scenarios in Set 2



= 0.8, the scenarios from C2-6 to C2-10 can be organized into two groups similar to those in Set 1 (C1-6 to C1-10). For example, if manufacturers place more importance on minimizing the average cycle time, they can choose C2-7 (322 min) and C2-10 (322 min), because the average cycle time drops significantly with both  $P_{25}$  and  $P_{50}$ . In terms of cost savings, C2-7 (\$697) can further offer better results with  $P_{25}$  to manufacturers compared to C2-10 (\$759). Also, if more weight is given to achieving minimum energy costs, manufacturers can select C2-8 (\$383), limiting the number of material extrusion machines working to the lowest possible level in the heating state with  $P_1$ . Moreover, C2-7 with  $P_{25}$  can provide a balanced combination of energy costs and average cycle time because the average cycle time decreases about 9157 min from C2-6 ( $P_1$ : 9,479 min) to C2-7 ( $P_{25}$ : 322 min), while energy costs rise only about \$311 from C2-6 ( $P_1$ : \$386) to C2-7 ( $P_{25}$ : \$697).

## 4 Conclusions

An AM energy simulation model of a production system with multiple material extrusion machines was proposed in this study based on MAR models to examine the trade-off between the average cycle time and energy costs. In particular, a set of experiments were conducted with two key process parameters (layer thickness and printing speed) to evaluate material extrusion power. A power model was developed as a linear function of MAR based on experimental results since MAR can represent layer thickness and printing speed as a single compound parameter. A theoretical facility with 50 material extrusion machines was simulated using the MAR regression model, and time series power profiles at the equipment and facility levels were obtained from the simulation model for 40 scenarios by changing production and simulation parameters.

Our proposed simulation model provides several beneficial results, as discussed in the illustrative examples, by showing how energy costs and cycle times of material extrusion can be controlled with various combinations of production parameters including machine control strategies. In particular, a balanced combination of average cycle time and energy costs can be obtained when a moderate number of machines are allowed to work at the same time. Also, manufacturers can choose one of the two controls policies between a reduced and an increased number of machines at the same time in the heating status, depending on their preference. On one hand, a reduced number of machines in the heating status result in reduced utility costs due to lower peak kilowatt and total kilowatt hour, but this strategy increased cycle time. On the other hand, an increase in the number of machines working in the heating status leads to improved cycle time, but this policy increased energy costs as well. Thus, manufacturers can benefit by employing a suitable control strategy during material extrusion. Also, the example analysis in this study showed that peak kilowatt and total kilowatt hour of material extrusion are relatively low when the volume of the printed parts is relatively small and there is less variability in the process.

Thus, results from our research can help industrial practitioners and academic researchers build a production strategy in such a way that a preferred amount of parts can be printed with acceptable energy costs. Our proposed energy simulation model can be applied to evaluate performance measures of a variety of AM methods. Also, a variety of time series energy data can be obtained using the simulation tool, data that can be used to forecast the electrical demand of AM facilities. Our method can be further extended to other related important research topics to study the power demand of material extrusion machines at the equipment and facility levels by performing extensive simulation runs with correlated process parameter settings. We expect to



address this point in future studies and to study research topics for generalizing the findings from  $P_1$ ,  $P_{25}$ , and  $P_{50}$  for other policies.

**Author contribution** Mohammad Rashidul Hassan: Study conceptualization, design, analysis, and manuscript writing. Heena Noh: Material preparation, experimental setup, and data collection. Kijung Park: Experiments, data collection, and manuscript review. Hyun Woo Jeon: Manuscript review and project supervision.

**Funding** This research was supported by the National Research Foundation of Korea (NRF) grant funded by the Korea government (MSIT) (No. NRF-2021R1G1A1091524).

**Availability of data and materials** The authors have no data and materials available to the public.

**Code availability** The authors have no code available to the public.

## Declarations

**Conflict of interest** The authors declare no competing interests.

## References

- Gibson I, Rosen DW, Stucker B (2010) Design for additive manufacturing. In Gibson I, Rosen DW, Stucker B (eds) Additive manufacturing technologies: rapid prototyping to direct digital manufacturing. Springer, US, Boston, MA, pp 299–332
- Mohamed OA, Masood SH, Bhowmik JL (2015) Optimization of fused deposition modeling process parameters: a review of current research and future prospects. *Adv Manuf* 3:42–53. <https://doi.org/10.1007/s40436-014-0097-7>
- (2015) ISO/ASTM 52900:2015. In *Addit Manuf Gen Princ Terminol ISO*. <https://www.iso.org/standard/69669.html>. Accessed 9 Jan 2021
- Singh S, Ramakrishna S, Singh R (2017) Material issues in additive manufacturing: a review. *J Manuf Process* 25:185–200. <https://doi.org/10.1016/j.jmapro.2016.11.006>
- Wohlers T, Campbell I, Diegel O et al (2021) Wohlers report 2021: 3D printing and additive manufacturing global state of the industry. Wohlers Assoc Fort Collins CO USA
- (2021) 3D Printing Market Size, Share, Industry Report, 2021–2028. <https://www.grandviewresearch.com/industry-analysis/3d-printing-industry-analysis>. Accessed: September 28, 2021
- (2015) National Grid, Understanding Electric Demand. [https://www.nationalgridus.com/niagaramohawk/non\\_html/eff\\_elec-demand.pdf](https://www.nationalgridus.com/niagaramohawk/non_html/eff_elec-demand.pdf). Accessed: November 4, 2020
- Wang Y, Li L (2015) Time-of-use electricity pricing for industrial customers: a survey of US utilities. *Appl Energy* 149:89–103. <https://doi.org/10.1016/j.apenergy.2015.03.118>
- Vyavahare S, Teraiya S, Panghal D, Kumar S (2020) Fused deposition modelling: a review. *Rapid Prototyp J* 176–201. <https://doi.org/10.1108/RPJ-04-2019-0106>
- Shaour B, Abuabiah M, Abdel-Fattah S et al (2021) Gaining a better understanding of the extrusion process in fused filament fabrication 3D printing: a review. *Int J Adv Manuf Technol* 114:1279–1291. <https://doi.org/10.1007/s00170-021-06918-6>
- Paul R, Anand S (2012) Process energy analysis and optimization in selective laser sintering. *J Manuf Syst* 31:429–437. <https://doi.org/10.1016/j.jmsy.2012.07.004>
- Mognol P, Lepicart D, Perry N (2006) Rapid prototyping: energy and environment in the spotlight. *Rapid Prototyp J* 12:26–34. <https://doi.org/10.1108/13552540610637246>
- Yang Y, Li L, Pan Y, Sun Z (2017) Energy consumption modeling of stereolithography-based additive manufacturing toward environmental sustainability. *J Ind Ecol* 21:S168–S178. <https://doi.org/10.1111/jieec.12589>
- Peng T, Yan F (2018) Dual-objective analysis for desktop FDM printers: energy consumption and surface roughness. 25th CIRP Life Cycle Eng LCE Conf 30 April – 2 May 2018 Cph Den 69:106–111. <https://doi.org/10.1016/j.procir.2017.11.084>
- Griffiths CA, Howarth J, De Almeida-Rowbotham G et al (2016) A design of experiments approach for the optimisation of energy and waste during the production of parts manufactured by 3D printing. *J Clean Prod* 139:74–85. <https://doi.org/10.1016/j.jclepro.2016.07.182>
- Lunetto V, Priarone PC, Galati M, Minetola P (2020) On the correlation between process parameters and specific energy consumption in fused deposition modelling. *J Manuf Process* 56:1039–1049. <https://doi.org/10.1016/j.jmapro.2020.06.002>
- Karimi S, Kwon S, Ning F (2021) Energy-aware production scheduling for additive manufacturing. *J Clean Prod* 278:123183. <https://doi.org/10.1016/j.jclepro.2020.123183>
- Elkaseer A, Schneider S, Scholz SG (2020) Experiment-Based process modeling and optimization for high-quality and resource-efficient FFF 3D printing. *Appl Sci* 10:2899. <https://doi.org/10.3390/app10082899>
- Hassan MR, Jeon HW, Kim G, Park K (2021) The effects of infill patterns and infill percentages on energy consumption in fused filament fabrication using CFR-PEEK. *Rapid Prototyp J ahead-of-print*: <https://doi.org/10.1108/RPJ-11-2020-0288>
- Xu X, Meteyer S, Perry N, Zhao YF (2015) Energy consumption model of binder-jetting additive manufacturing processes. *Int J Prod Res* 53:7005–7015. <https://doi.org/10.1080/00207543.2014.937013>
- Jeon HW, Lee S, Wang C (2019) Estimating manufacturing electricity costs by simulating dependence between production parameters. *Robot Comput-Integr Manuf* 55:129–140. <https://doi.org/10.1016/j.rcim.2018.07.009>
- Ding J (2021) Energy aware scheduling in flexible flow shops with hybrid particle swarm optimization. *Comput Oper Res* 17. <https://doi.org/10.1016/j.cor.2020.105088>
- Han X, Yang D, Yang C et al (2019) Carbon fiber reinforced PEEK composites based on 3D-printing technology for orthopedic and dental applications. *J Clin Med* 8:240. <https://doi.org/10.3390/jcm8020240>
- Popescu D, Zapciu A, Amza C et al (2018) FDM process parameters influence over the mechanical properties of polymer specimens: a review. *Polym Test* 69:157–166. <https://doi.org/10.1016/j.polymertesting.2018.05.020>
- Qin X, Wu X, Li H et al (2021) Numerical and experimental investigation of orthogonal cutting of carbon fiber-reinforced polyetheretherketone (CF/PEEK). *Int J Adv Manuf Technol*. <https://doi.org/10.1007/s00170-021-08317-3>
- Park K, Kim G, No H et al (2020) Identification of optimal process parameter settings based on manufacturing performance for fused filament fabrication of CFR-PEEK. *Appl Sci* 10:4630. <https://doi.org/10.3390/app10134630>
- El Magri A, Vanaei S, Vaudreuil S (2021) An overview on the influence of process parameters through the characteristic of 3D-printed PEEK and PEI parts. *High Perform Polym* 1–19. <https://doi.org/10.1177/09540083211009961>

28. Deng X, Zeng Z, Peng B et al (2018) Mechanical properties optimization of poly-ether-ether-ketone via fused deposition modeling. *Materials* 11:216. <https://doi.org/10.3390/ma11020216>
29. van de Werken N, Koirala P, Ghorbani J et al (2021) Investigating the hot isostatic pressing of an additively manufactured continuous carbon fiber reinforced PEEK composite. *Addit Manuf* 37:101634. <https://doi.org/10.1016/j.addma.2020.101634>
30. Gutowski TG, Branham MS, Dahmus JB et al (2009) Thermodynamic analysis of resources used in manufacturing processes. *Environ Sci Technol* 43:1584–1590. <https://doi.org/10.1021/es8016655>
31. Diaz N, Redelsheimer E, Dornfeld D (2011) Energy consumption characterization and reduction strategies for milling machine tool use. In Hesselbach J, Herrmann C (eds) *Glocalized Solutions for Sustainability in Manufacturing*. Springer, Berlin Heidelberg, Berlin, Heidelberg, pp 263–267
32. Zhu Z, Dhokia VG, Nassehi A, Newman ST (2013) A methodology for the estimation of build time for operation sequencing in process planning for a hybrid process. In *Advances in Sustainable and Competitive Manufacturing Systems*. Springer, pp 159–171
33. Komineas G, Foteinopoulos P, Papacharalampopoulos A, Stavropoulos P (2018) Build time estimation models in thermal extrusion additive manufacturing processes. *Procedia Manuf* 21:647–654. <https://doi.org/10.1016/j.promfg.2018.02.167>
34. Kose H, Jin M, Peng T (2020) Quality and productivity trade-off in powder-bed additive manufacturing. *Prog Addit Manuf* 1–12. <https://doi.org/10.1007/s40964-020-00122-w>
35. Ekren BY (2020) A simulation-based experimental design for SBS/RS warehouse design by considering energy related performance metrics. *Simul Model Pract Theory* 98:101991. <https://doi.org/10.1016/j.simpat.2019.101991>
36. Nshama EW, Msukwa MR, Uchiyama N (2021) A Trade-off between energy saving and cycle time reduction by pareto optimal corner smoothing in industrial feed drive systems. *IEEE Access* 9:23579–23594. <https://doi.org/10.1109/ACCESS.2021.3056755>
37. (2021) Simio 14. In Simio Version 1422123179. <https://www.simio.com/resources/release-notes/notes/Version-14-summary.php>. Accessed 17 Dec 2021
38. (2017) MATLAB R2017b. In MATLAB Doc. <https://www.mathworks.com/help/releases/R2017b/matlab/index.html>. Accessed 5 Jan 2022
39. (2019) Apium. In Apium P220 Datasheet. <https://apiumtec.com/download/apium-p220-datasheet>. Accessed 19 Feb 2021
40. (2018) Apium. In Apium CFR PEEK Data-Sheet. <https://apiumtec.com/download/apium-cfr-peek-datasheet>. Accessed 19 Feb 2021
41. Ensinger (2021) PEEK carbon fibre reinforced - TECAPEEK CF30 black. <https://www.ensingerplastics.com/en/shapes/products/peek-tecapeek-cf30-black>. Accessed 14 Sep 2021
42. (2021) Wattman (HPM-100A). In ADPower. <http://shop2.adpower21.com.cafe24.com/product/wattman-hpm-100a/17>. Accessed 19 Feb 2021
43. (2021) Simplify3D. In Simpl. Version 410. <https://www.simplify3d.com/software/release-notes/version-4-1-0/>. Accessed 19 Feb 2021
44. Yamamoto BE, Trimble AZ, Minei B, Ghasemi Nejjad MN (2019) Development of multifunctional nanocomposites with 3-D printing additive manufacturing and low graphene loading. *J Thermoplast Compos Mater* 32:383–408. <https://doi.org/10.1177/2F0892705718759390>
45. Xu F, Loh H, Wong Y (1999) Considerations and selection of optimal orientation for different rapid prototyping systems. *Rapid Prototyp J* 54–60. <https://doi.org/10.1108/13552549910267344>
46. (2021) Slic3r Manual – Cooling. <https://manual.slic3r.org/expert-mode/cooling>. Accessed 14 Jul 2021
47. Prabhu VV, Jeon HW, Taisch M (2012) Modeling green factory physics - an analytical approach. In 2012 IEEE International Conference on Automation Science and Engineering (CASE). IEEE, Seoul, Korea (South), pp 46–51
48. Shortle JF, Thompson JM, Gross D, Harris CM (2018) *Fundamentals of queueing theory*, 5th edn. John Wiley & Sons
49. Wolff RW (1989) *Stochastic modelling and the theory of queues*. Englewood Cliffs NJ 96
50. Prabhu VV, Jeon HW, Taisch M (2013) Simulation modelling of energy dynamics in discrete manufacturing systems. In *Service orientation in holonic and multi agent manufacturing and robotics*. Springer, pp 293–311

**Publisher's note** Springer Nature remains neutral with regard to jurisdictional claims in published maps and institutional affiliations.